

CIRCUMSTELLAR Na I AND Ca II LINES OF TYPE Ia SUPERNOVAE IN SYMBIOTIC SCENARIO

N. N. Chugai

Institute of Astronomy, RAS, Pyatnitskaya 48, 119017 Moscow, Russia

nchugai@inasan.ru

ABSTRACT

Formation of circumstellar resonant lines of Na I and Ca II in type Ia supernovae is studied for the case, when supernova explodes in a binary system with a red giant. The model suggests a spherically-symmetric wind and takes into account ionization and heating of the wind by X-rays from the shock wave and by gamma-quanta of ^{56}Ni radioactive decay. For the wind density typical of the red giant the expected optical depth of the wind in Na I lines turns out low ($\tau < 10^{-3}$) to detect the absorption. For the same wind densities the predicted optical depth of Ca II 3934 Å is sufficient for the detection ($\tau > 0.1$). I conclude that the absorption lines detected in SN 2006X cannot form in the red giant wind; they are rather related to clouds at distances larger than the dust evaporation radius ($r > 10^{17}$ cm). From the absence in SN 2006X of Ca II absorption lines not related with the similar Na I components I derive the upper limit of the mass loss rate by the wind with velocity u : $\dot{M} < 10^{-8}(u/10 \text{ km s}^{-1}) M_{\odot} \text{ yr}^{-1}$.

1. INTRODUCTION

Thermonuclear supernovae (SN Ia) are the result of explosion of carbon-oxygen white dwarf that attains the Chandrasekhar mass of $1.4 M_{\odot}$ due to mass accretion in a binary system (Wheelan & Iben 1973). The question, which types of binaries are responsible for SN Ia, remains a subject of debates. A supernova explosion in a symbiotic system ("symbiotic scenario") in which a donor is a red giant is among possible options (Tutukov & Yungelson 1976; Iben & Tutukov 1984; Hachisu & Kato 2000). This scenario is a subject of a special interest because of the possibility of observational tests.

One of the outcomes of the symbiotic scenario might be the presence of the red giant matter in the SN Ia envelope (Chugai 1986; Livne et al. 1992; Marietta et al. 2000) which could be observed as a narrow H α emission at the nebular stage. Until now this line has not

been detected. More obvious consequence of the symbiotic scenario would be the presence of a slow red giant wind. The wind could be revealed through the radio and X-ray emission originated from the supernova expansion in the circumstellar (CS) gas. The search in radio (Panagia et al. 2006) and X-ray (Hughes et al. 2007) bands provides as yet only an upper limit of fluxes. The signature of the red giant wind could be present at the early stage of supernova in the optical as the narrow $H\alpha$ emission, which however also has not been found as yet (Cumming et al. 1996). Finally, the red giant wind could be in principle observed as variable CS Na I and Ca II absorption lines with radial velocities of several tens of km s^{-1} against the SN Ia quasicontinuum.

Recently, Patat et al. (2007) detected variable Na I 5890, 5896 Å absorption lines with low expansion velocities in the spectrum of SN 2006X, a normal type Ia supernova. These absorptions being identified with a red giant wind compose a serious argument in favour of the symbiotic scenario at least in the particular case of SN 2006X (Patat et al. 2007). Given both the importance of this result and the fact that the formation of the CS absorption lines of Na I and Ca II in the red giant wind after SN Ia explosion has not been studied until now, it would be of interest to understand what is the expected intensity of these lines in the symbiotic scenario and whether these line could be observable.

Here I propose a simple model to describe physical conditions in the red giant wind after the SN Ia explosion, which eventually would permit us to calculate intensities of CS absorption lines of Na I and Ca II against the supernova background. I start with the analysis of physical conditions in the preexplosion wind (section 2.1). I then calculate temperature and ionization of the wind after the supernova explosion using time-dependent model and taking into account absorption of X-rays from shock wave and Compton scattering of gamma-quanta from radioactive ^{56}Ni decay (section 2.2). This provides us a possibility to find the ionization fraction of Na I and Ca II and the optical depth in resonant lines of these ions as a function of time (section 2.3). In the last section I discuss the observational test for the symbiotic scenario of SN Ia and compare results with observations of these lines in SN 2006X.

2. MODEL AND RESULTS

Modeling of circumstellar Na I and Ca II lines in SN Ia spectra in a context of the symbiotic scenario suggests generally a solution of two problems: (1) determination of an initial state of the CS gas before the supernova explosion and (2) calculation of conditions in the wind after the supernova explosion. In fact, as we will see below, the first issue is of little significance for the final result. Nevertheless we will consider this problem using simple models of the wind and the central source of ionizing radiation in the symbiotic system. The

second problem is by far more important for the final result and its solution requires the consideration of all the essential physics of the wind ionization and heating as well as of the ionization of Na I and Ca II.

2.1. Wind before supernova explosion

Red giant wind properties in the symbiotic scenario of SN Ia are poorly known; even for the well studied galactic symbiotic binaries the mass-loss rate is determined with a large uncertainty. The mass-loss rate estimates lie in the range of $10^{-8} - 10^{-6} M_{\odot} \text{ yr}^{-1}$ (Korreck et al. 2007), while the wind velocities are in the range of 10–50 km s⁻¹. We adopt below the wind velocity $u = 30 \text{ km s}^{-1}$. An orbital motion and a fast bipolar wind from the disk can result in asphericity of the slow wind outside the binary orbit. We, however, consider a stationary spherical wind with the density $\rho = w/4\pi r^2$. Results obtained for this model could be used also to estimate conditions in the CS gas with a more complex structure. It is convenient to deal with the parameter ω defined by the relation $w = 6.3 \times 10^{13} \omega \text{ g cm}^{-1}$. The mass loss rate in terms of ω is $\dot{M} = 10^{-6} \omega u_{10} M_{\odot} \text{ yr}^{-1}$, where u_{10} is the wind velocity in units of 10 km s⁻¹.

Before the supernova explosion the hydrogen in the wind is ionized by the radiation of an accretion disk, white dwarf and partially by the radiation of the red giant. We facilitate the model assuming a single spherical source of the black body radiation with the temperature $T_s = 30000 \text{ K}$ and luminosity $L_s = 300L_{\odot}$; these parameters are similar to those of the symbiotic recurrent nova RS Oph between outbursts (Dobrzycka et al 1996). Depending on the radial extent of the Strömgen zone the wind is fully or partially ionized. In order to model ionization in the partially ionized wind we adopt two levels plus continuum approximation. In this case the ionization can occur primarily via the two-stage process: excitation of the second level by the radiation of the central source with the subsequent photoionization from the second level. The $L\alpha$ radiation transfer is treated in the frame of a simple probability approach, which is widely used in the modelling of spectra of active galaxies (Collin-Souffrin & Dumont 1989). The escape probability for $L\alpha$ quanta is adopted to be $\beta_{12} = 1/(1 + \tau_{12})$, where $\tau_{12} = \tau_{12,\text{in}} + \tau_{12,\text{out}}$, $\tau_{12,\text{in}}$ is the optical distance of a given point of the wind from the inner wind boundary, while $\tau_{12,\text{out}}$ is the optical distance from a given point to the outer boundary of the wind. The excitation rate of the second level is determined by the probability $\beta_{12,\text{in}} = 1/(1 + \tau_{12,\text{in}})$.

The hydrogen ionization is calculated using a steady-state approximation in the inner zone, where stationary approximation is valid, and using time-dependent model in the outer zone. Taking into account the fact that the photoionization rate for the excited level steeply

decreases with the radius ($P \propto r^{-4}$) and gets essentially small at large radii it would be of interest to consider a simple recombination model that includes only expansion and recombination. Assuming a constant temperature the equation for the electron concentration in the co-moving frame reads

$$\frac{dn_e}{dr} = -\frac{2n_e}{r} - an_e^2, \quad (1)$$

where $a = \alpha/u$ (α is the recombination coefficient). Solving the equation analytically with the boundary condition $x = n_e/n = x_0$ at the inner radius r_0 and taking account of the hydrogen concentration $n = n_0(r_0/r)^2$ we find the ionization fraction for $r > r_0$

$$x = x_0 \left(\frac{r}{r_0} \right) \left[(1 + \xi) \left(\frac{r}{r_0} \right) - \xi \right]^{-1}, \quad (2)$$

where $\xi = \alpha x_0 n_0 r_0 / u$ is stationary ionization parameter. For $r \gg r_0$ the ionization fraction asymptotically approaches the constant value $x = x_0 / (1 + \xi)$, i.e. a freeze-out occurs (Zeldovich & Raizer 2002). The photoionization from the second level somewhat changes this simple relation.

The calculated ionization fraction in the model with the temperature distribution $T = T_s W^{1/4}$, where W is the dilution factor, is plotted in Fig. 1 for two values of the density parameter ω (0.1, and 1). In the range $r > 10^{14}$ cm the ionization fraction does not exceed 10^{-2} . The weak dependence $x(r)$ in the outer zone $r > 10^{15}$ cm reflects the freeze-out effect considered above. For $\omega = 1$ the ionization fraction at large distances attains 10^{-4} . In this case the electron concentration is comparable with the contribution of singly ionized metals (Mg, Si, Fe). For the rarefied wind $\omega = 0.01$ the gas is fully ionized. In this case we adopt $x = 1$ and $T_e = 10^4$ K. Hereafter we take into account only two ions for Na and Ca (Na I, Na II and Ca II, Ca III respectively). This is justified by the high ionization potential of Na II (47 eV), which makes the role of Na III negligible. In the case of Ca the situation is opposite: the low ionization potential of Ca I (6.1 eV) results in the negligibly low concentration of Ca I, which does not affect the fraction of Ca II. In all three cases of the wind density the ratio Na I/Na turns out to be of the order of $\xi_{\text{Na,I}} \sim 10^{-4}$, while the ratio Ca II/Ca is close to unity ($\xi_{\text{Ca,2}} \approx 1$). The calculated preexplosion ionization fraction of hydrogen, sodium and calcium are substantially modified after the explosion.

2.2. Wind after explosion

The wind ionization and heating after SN Ia explosion can be produced by (1) absorption of the ultraviolet (UV) supernova radiation; (2) absorption of the X-rays emitted by the reverse shock originated from the deceleration of the supernova in the wind; (3) Compton

scattering of gamma-rays from ^{56}Ni - ^{56}Co - ^{56}Fe radioactive decay. The possibility of the wind ionization around SN 2006X by X-rays has been already invoked for the interpretation of the CS absorption lines (Patat et al. 2007), while the role of gamma-rays in the wind ionization has never been discussed. The hydrogen photoionization is not efficient, because the emergent supernova radiation is strongly suppressed in the UV band due to metal line opacity. Estimates based on the model UV spectrum of SN Ia (Pauldrach et al. 1996) show that even in the light maximum the supernova radiation cannot ionize the hydrogen in the wind. However, the photoionization of NaI and CaII is of crucial importance and will be taken into account.

Interaction of a supernova envelope with a wind results in the formation of a double shock structure consisting of the forward shock in the wind and the reverse shock in the supernova ejecta. For the expected wind densities ($\omega \leq 1$) X-rays from the reverse shock dominate. To calculate the X-ray luminosity we use a self-similar solution describing ejecta deceleration in the wind (Chevalier 1982; Nadyozhin 1985). The density distribution in the undisturbed ejecta is assumed to be power law $\rho \propto v^{-k}$ in the outer layers ($v > v_0$) and homogeneous inside ($v < v_0$). We use $k = 9$ which reproduces the initial deceleration, computed for the realistic ejecta density distribution. Parameter v_0 is determined by the supernova kinetic energy and mass which are adopted to be $E = 1.4 \times 10^{51}$ erg and $M = 1.4 M_\odot$ respectively. The density in the reverse shock wave is assumed to be constant, while the shock width is taken to be $\Delta R = 0.03R$ (Chevalier 1982). For the relevant conditions Coulomb collisions are not able to equilibrate electron and ion temperatures, so we adopt rather arbitrary $T_e = 0.1T_i$. Variations of the T_e/T_i ratio do not affect seriously final results.

Of the absorbed X-ray energy the fraction $\eta_h \approx x^{0.24}$ is spent on heating (cf. Kozma & Fransson 1992). The rest of the absorbed energy is distributed equally between hydrogen ionization and excitation so that the efficiency of the hydrogen ionization is $\eta_i = 0.5(1 - \eta_h)$. In addition, some fraction of the deposited energy is spent on the two-stage ionization via the excitation by secondary electrons and subsequent photoionization by the supernova radiation. The probability of this channel is $\phi_2 = P_2/(P_2 + A_{21}\beta_{12} + A_{2q})$, where P_2 is the photoionization rate, $A_{21}\beta_{12}$ is the L α escape rate, and A_{2q} is the two-photon decay probability. Given the deposition rate ϵ (erg cm $^{-3}$ s $^{-1}$), the ionization rate is then $\eta_i(1 + \phi_2)\epsilon/\chi$, where χ is the hydrogen ionization potential. We assume that equilibration of electron and ion temperatures in the wind occurs quickly, — an acceptable approximation for the wind density $> 10^4$ cm $^{-3}$. For instance, assuming $n \sim 10^4$ cm $^{-3}$ and $T_e = 4 \times 10^5$ K the equilibration time is $t_{\text{eq}} \sim 3$ days. Radiative cooling is described in terms of the cooling function which is taken according to Sutherland & Dopita (1993). Additionally, we take into account the Compton cooling due to photons scattering off the wind electrons; this mechanism can contribute markedly in the gas cooling for $T_e \geq 10^5$ K.

Wind ionization and heating by gamma-rays of the radioactive decay is calculated in the approximation of a single scattering which is treated as an absorption with the effective absorption coefficient $k = \alpha k_T$ (where k_T is the absorption coefficient due to Thomson scattering). The average value of α in the range of 0.2–2 MeV is about 0.12 (Sutherland & Wheeler 1984). With this value of α the gamma-ray absorption coefficient is $k \approx 0.04 \text{ cm}^2 \text{ g}^{-1}$. The fraction of the escaping gamma-ray luminosity $q(t)$ was calculated for a set of SN Ia models by Höflich et al. (1993). We approximate this computations by the "average" analytical expression

$$q(t) = 0.05 \exp[-(t_1/t)^2] + 0.95 \exp[-(t_2/t)^2], \quad (3)$$

where $t_1 = 20 \text{ d}$ and $t_2 = 36 \text{ d}$. The initial mass of radioactive ^{56}Ni is taken to be $0.55 M_\odot$ in accordance with the empirical bolometric light curves of SN Ia (cf. Wang et al. 2007).

The ionization fraction and the gas temperature are calculated via numerical solution of time-dependent ionization equations in the two-level plus continuum approximation and a time-dependent thermal balance equation. An example of the radial distribution of the electron temperature and hydrogen ionization fraction in the preshock wind on day 30 after the supernova explosion is shown in Fig. 2 for the case of $\omega = 0.1$. The values of x and T_e decrease with the radius approximately as r^{-2} . In the shock wave proximity $T_e \sim 10^5 \text{ K}$ whereas at the distance 10^{17} cm the temperature drops down to $\sim 10^3 \text{ K}$. Note, the ionization fraction in the wind is substantially higher than before the supernova explosion (cf. Fig. 1).

The relative contribution of the shock X-rays and gamma-rays of radioactive decay in the heating and therefore in the ionization is demonstrated qualitatively in Fig. 3 which shows evolution of the temperature in the preshock zone. At the early epoch ($t < 15 \text{ d}$) X-rays dominate in the heating, while the gamma-rays dominate at the later epoch, at least until day 400. The temperature maximum at about 50 d being apparent for $\omega = 0.01$ and $\omega = 0.1$ is related to the maximum of luminosity of escaping gamma-rays (inset in Fig. 3).

2.3. Intensity of Na I and Ca II lines after supernova outburst

The primary ionization mechanism for Na I and Ca II after the SN Ia explosion is the photoionization from the ground and excited states. The specific feature of these ions is the low photoionization cross section for the ground level. The role of the two-stage process — the excitation and subsequent photoionization from the excited level — is, therefore, of high importance. The latter is especially apparent for Na I because the UV radiation of SN Ia is strongly suppressed, while the two-stage ionization operates via the visible radiation. We assume the spectrum of SN Ia to be black body with the temperature of 10000 K, but with

the suppressed UV flux. The time-independent, but wavelength-dependent, UV suppression factor is derived from the synthetic and observed spectrum of SN 1992A at the light maximum (Pauldrach et al. 1996). The bolometric light curve of SN Ia is taken according to the observationally recovered bolometric luminosity (Wang et al. 2007). The Na I and Ca II ionization is considered in the two-level plus continuum approximation. The photoionization cross sections for the ground level are taken from Verner et al. (1996), while the photoionization cross sections for excited levels are assumed to be hydrogenic. The ionization fraction of Na I and Ca II is found by numerical solution of time-dependent equation of ionization balance on the background of the calculated ionization and temperature of the wind.

After the supernova outburst the Na I photoionization dominates and therefore the Na I concentration drops exponentially $dn_1/dt \approx -Pn_1$, where P is the photoionization rate. When the photoionization from the excited level is dominant the ionization rate is $P \sim 10^5 W^2 \sim 10 \text{ s}^{-1}$, assuming the dilution factor $W = 0.01$. On the other hand, the recombination rate $\alpha n_e \sim 4 \times 10^{-8} \text{ s}^{-1}$ adopting $n_e = 10^5 \text{ cm}^{-3}$, i.e. by the eight orders lower. This explains why the Na I fraction is small and does not exceed $\xi_{\text{Na},1} \sim 10^{-8}$ on day 30 (Fig. 4). The Ca II photoionization is less efficient so the Ca II fraction in the inner zone is $\xi_{\text{Ca},2} \sim 10^{-4} - 10^{-2}$, while in the outer zone $r > 10^{17} \text{ cm}$ approaches unity.

Evolution of the optical depth in resonant Na I Ca II lines on the background of the expanding supernova is shown in Fig. 5 for three values of the wind density parameter. Inset shows the evolution of the radius of the supernova-wind interface which is the lower limit for the integration of the optical depth in CS lines. When computing the line absorption coefficient we used the Doppler width $u_D = 10 \text{ km s}^{-1}$. The major conclusion from the presented results is the low optical depth of the wind in the Na I 5890 Å line ($\tau < 10^{-3}$) and rather high optical depth in the Ca II 3934 Å line ($\tau > 0.1$). For the same wind density the optical depth in Ca II line is by four orders larger than that in Na I. Interestingly, even for the rarefied wind ($\omega = 0.01$) the optical depth in the Ca II 3934 Å line at the early epoch $t \leq 10 \text{ d}$ exceeds unity. These results do not depend on the physical conditions in the pre-explosion wind since the photoionization and heating after the supernova explosion quickly washes out the initial conditions.

Model uncertainties could affect the calculated Na I optical depth, although corrections are unlikely exceed the factor of two. Remarkably, results for Na I are not sensitive to the uncertainty of UV spectrum of SN Ia because the quanta responsible for the photoionization from the excited level are distributed in the visible range $\lambda > 3500 \text{ Å}$. The latter statement is not valid for Ca II because the radiation responsible for the ionization from excited level comes from UV band ($h\nu \sim 8 - 9 \text{ eV}$). Yet, since the UV spectrum used in our model is based on the observational and synthetic spectrum of SN Ia, the uncertainty of UV spectrum

unlikely markedly change the optical depth in the Ca II line compared to the above results.

Of special interest is a model with a dense shell on the background of a wind of a moderate density $\omega = 0.1$. In the considered example the shell with the width $\Delta r = 0.1r$ is placed at the distance $r = 6 \times 10^{16}$ cm. The density of the shell is chosen to make the optical depth of Na I 5890 Å close to unity on day 30. It was found that this condition requires the shell mass of $\approx 0.5 M_{\odot}$. The evolution of the optical depth in Na I and Ca II lines and the fractions of Na I and Ca II are shown in Fig. 6. This model could relate to the interpretation of the CS lines of Na I and Ca II in SN 2006X.

3. DISCUSSION AND CONCLUSION

The aim of the paper has been to calculate the intensity of CS resonant absorption lines of Na I and Ca II in the spectrum of SN Ia in the frame of symbiotic scenario. The modelling shows that for the wind densities typical of a red giant, $\omega \sim 0.01 - 1$, the expected optical depth in the Na I 5890 Å line is very low, $\tau < 10^{-3}$. The slow wind around symbiotic binary, therefore, unlikely can be detected in the absorption Na I lines on the background of SN Ia. On the other hand, the model predicts for the same CS densities rather strong Ca II 3934 Å absorption line with $\tau > 0.1$. At the early time $t \leq 10$ d the optical depth in the Ca II 3934 Å line can exceed unity even in the case of rarefied wind $\omega = 0.01$. It is reasonable, therefore, to search for the signatures of the red giant wind in the Ca II 3934, 3968 Å lines close to the light maximum.

The modelling of the circumstellar Na I and Ca II lines in the red giant wind are of particular interest in relation to the observations of these lines in SN 2006X. In the spectra of this supernova four low velocity variable components (A, B, C, D) in Na I lines has been found (Patat et al. 2007). Two (A and B) are observed simultaneously in both Na I lines and Ca II 3934 Å line, while C and D components are seen only in Na I lines. Remarkably, in the spectrum of SN 2006X one does not detect any absorption components of Ca II with the depth ≥ 0.2 , which is not seen in Na I lines (cf. Patat et al. 2007). This fact, according to our modelling (Fig. 5), indicates that the wind density around SN 2006X is low, $\omega < 0.01$. The corresponding upper limit on the mass loss rate is $\dot{M} < 10^{-8} u_{10} M_{\odot} \text{ yr}^{-1}$.

A question arises as to the origin of the Na I and Ca II absorption lines detected in SN 2006X. Components C and D, observed in Na I lines strengthen between days -2 and +14 relative the light maximum, or in the range $16 < t < 32$ d after the explosion (assuming maximum at $t = 18$ d) and disappear on day 79 (Patat et al. 2007). The disappearance of C and D components might indicate that they form in a relatively close $r \sim 10^{16}$ cm dense shell

that is accelerated between days 32 and 79 by the supernova ejecta (Patat et al. 2007). A problem with this scenario is the absence of absorption components C and D in the Ca II line. Taking into account that in our model the Na I line is by 3–4 orders of magnitude weaker than the Ca II line one needs to admit that the latter is strongly suppressed somehow by 4–5 orders of magnitude. A reasonable possibility might be depletion of Ca onto dust grains. In fact, in the interstellar medium the Ca depletion factor can be as low as 10^{-3} – 10^{-4} (Krinklow et al. 1994). However, in the case of C and D components this explanation faces a serious difficulty. The point is that even the heavy depletion of Ca were the case, the dust would evaporate after the supernova explosion. Indeed, assuming the grain absorption efficiency $Q_a \propto 1/\lambda$, supernova luminosity 10^{43} erg s $^{-1}$, and the supernova radiation temperature $T = 10^4$ K one gets the dust temperature $T_d = W^{1/5}T \approx 2600$ K at the radius 1.5×10^{16} cm. The derived dust temperature is substantially higher than the evaporation temperature (~ 1000 K). This implies that the shell with the radius of $\sim 10^{16}$ seems to be not viable model for the C and D components.

The second pair of components, A and B, which are seen in both Na I and Ca II is presumably related with the distant shell (Patat et al. 2007), because on day 139 the lines retain the same intensity as at the previous epoch. For the wind density parameter $\omega = 0.1$ the radius of SN-wind interface suggests that the shell radius should be $r > 4 \times 10^{16}$ cm (cf. Fig. 5). The model of the Na I and Ca II line formation in the shell with the radius of 6×10^{16} cm illustrates this possibility. However in this case the shell mass should be rather large, $\approx 0.5 M_\odot$. The origin of this shell is a not a trivial problem. As a possibility one could speculate that the shell has been ejected as a result of a robust dynamical mass loss episode.

Difficulties of the interpretation of Na I and Ca II absorption lines in the SN 2006X spectrum in the model of the CS wind push us to an alternative view, which suggests that these lines originate beyond the dust evaporation radius $r > 10^{17}$ cm. This conjecture permits us to explain why Ca II lines are not seen in components C and D. In this case the variability of the Na I line depth is presumably caused by the variation of occultation by clouds of the expanding supernova "photosphere". The model of variable covering factor due to the photosphere expansion was already discussed and rejected by Patat et al. (2007) because A and B components of Ca II line did not show simultaneous variability. However, the latter argument loses its strength, if there are clouds of two types: (1) "ordinary" clouds in which Ca is not depleted, with the weak Na I and strong Ca II lines; (2) dense dusty clouds in which Na I lines are strong but Ca II lines are suppressed owing to Ca depletion onto dust grains. In this case the behavior of Ca II and Na I lines can be independent with the Ca II lines being constant, and Na I being variable; the latter, e.g., because the early supernova photosphere is not covered by the second sort of clouds.

Components C and D which are seen only in Na I line could be explained in a similar way; in this case however only clouds of second variety are needed. Since C and D components do not show Ca II lines these clouds should be dusty in order to deplete Ca and be at distances larger than the dust evaporation radius. The evolution of components C and D in Na I lines could be explained in the following way. At the beginning, when the photosphere radius is small, the supernova is seen presumably through the hole of some cluster of clouds. The supernova photosphere while expanding gets occulted by clouds so the covering factor increases. Assuming that the cloud cluster occupies a finite solid angle in the sky plane one comes to the picture when a subsequent expansion of the photosphere would result in the covering factor decrease. The performed modelling shows that the required evolution of components C and D can be reproduced, e.g., by the cluster of four clouds with a typical cloud radius of $\sim 1.3 \times 10^{15}$ cm.

The origin of absorbing clouds at the radii $r > 10^{17}$ cm is unclear. They may originate from the matter lost by the binary system in which SN 2006X exploded. Alternatively they may not be related to the presupernova of SN 2006X at all. In this regard it is noteworthy that SN 2006X shows unusually high reddening $E(B - V) \approx 1.4$ (Wang et al. 2007). The presence of large amount of clouds in the line of sight might create a favourable condition for the variability of Na I and Ca II lines. If so, one could expect the similar variability of Na I and Ca II lines in other cases of SN Ia with heavy reddening. It should be emphasised that clouds responsible for the variation of Na I and Ca II lines provide only small fraction of the total dust absorption. This follows from the equivalent width of A, B, C, and D components of Na I line, which is a small fraction of total equivalent width of the Na I absorption line in our and host galaxies (Patat et al. 2007).

Summing up, a signature of a red giant wind around SN Ia exploded in a symbiotic binary will be unlikely observable in the Na I absorption lines, while the Ca II absorption lines can be detectable. The absence in the SN 2006X spectrum of the Ca II absorption lines which are not related with the similar components of Na I lines implies the upper limit on the mass loss rate $\dot{M} < 10^{-8} u_{10} M_{\odot} \text{ yr}^{-1}$. The absorption lines of Na I and Ca II observed in SN 2006X are related probably with distant clouds at the radii $r > 10^{17}$ cm.

4. Acknowledgements

I am grateful to Nando Patat for discussions.

REFERENCES

- Chevalier R.A. *Astrophys. J.*, **259**, 302 (1982).
- Chugai N.N. *Sov. Astronomy*, **30**, 563 (1986).
- Collin-Souffrin S., Dumont A.M. *Astron. Astrophys.*, **213**, 29 (1989).
- Crinklaw G., Federman S.R., Joseph C.L. *Astrophys. J.*, **424**, 748 (1994).
- Cumming R.J., Lundqvist P., Smith L.J. et al. *Mon. Not. R. astron. Soc.*, **283**, 1355 (1996).
- Dobrzycka D., Kenyon S.J., Proga D. et al. *Astron. J.*, **111**, 2090 (1996).
- Hachisu I., Kato M. *Astrophys. J.*, **536**, L93 (2000)
- Hoeflich P., Mueller E., Khokhlov A. *Astron. Astrophys. Suppl.*, **97**, 221 (1993).
- Hughes J.P., Chugai N., Chevalier R. et al. *Astrophys. J.*, **670**, 1260 (2007).
- Iben I., Tutukov A.V. *Astrophys. J. Suppl.*, **54**, 335 (1984).
- Korreck K.E., Kellogg E., Sokoloski J.L. The multicolored landscape of compact object objects and their explosive origins. *AIP Conference Proceedings*, v. 924, p. 903 (2007).
- Kozma C., Fransson C. *Astrophys. J.*, **390**, 602 (1992).
- Livne E., Tuchman Y., Wheeler C.J., *Astrophys. J.* **399**, 665 (1992).
- Marietta E., Burrows A., Fryxell B., *Astrophys. J. Suppl.*, **128**, 615 (2000).
- Nadyozhin D.K. *Astrophys. Space Sci.*, **112**, 225 (1985).
- Panagia N., Van Dyk S.D., Weiler K.W. et al. *Astrophys. J.*, **646**, 369 (2006).
- Patat F., Chandra P., Chevalier R. et al. *Science*, **315** 924 (2007).
- Pauldrach A.W.A., Duschinger M., Mazzali P.A. et al. *Astron. Astrophys.*, **312**, 525 (1996).
- Sutherland R.S., Dopita M.A. *Astrophys. J. Suppl.*, **88**, 253 (1993).
- Sutherland P.G., Wheeler J.C. *Astrophys. J. Suppl.*, **280**, 282 (1984).
- Tutukov A.V., Yungelson L.R. *Astrophysics*, **12**, 342 (1976)
- Verner D.A., Ferland G.J., Korista K.T., Yakovlev D.G. *Astrophys. J.*, **465**, 487 (1996).

Wang X., Li W., Filippenko A.V. et al. arXiv: 0708.0140 (2007).

Whelan J., Iben I. *Astrophys. J.*, **186**, 1007 (1973).

Zeldovich Ya. B., Raizer Yu.P. *Physics of shock waves and high temperature hydrodynamic phenomena*. Dover Publications. (2002).

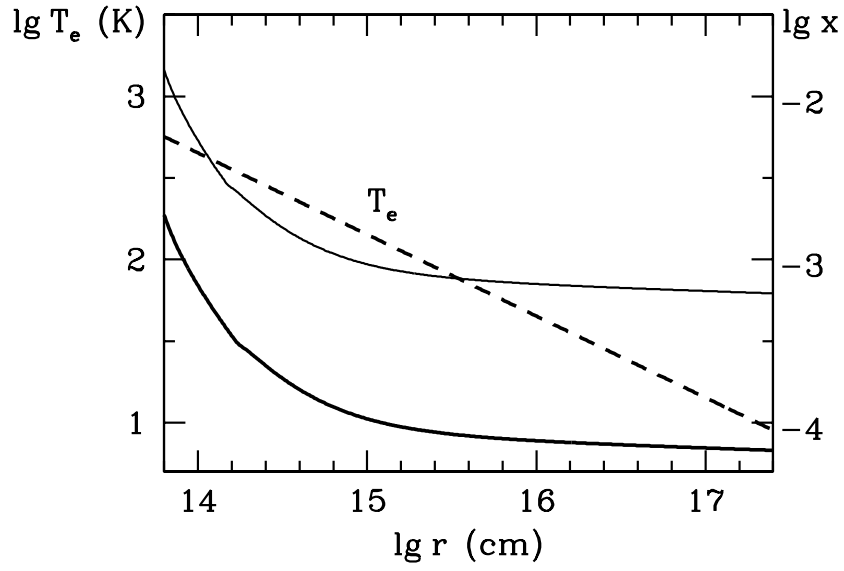


Fig. 1.— Ionization fraction and temperature in the wind prior to supernova explosion for two values of the wind density parameter $\omega = 0.01$ and $\omega = 0.1$. The thinnest line refers to lower density

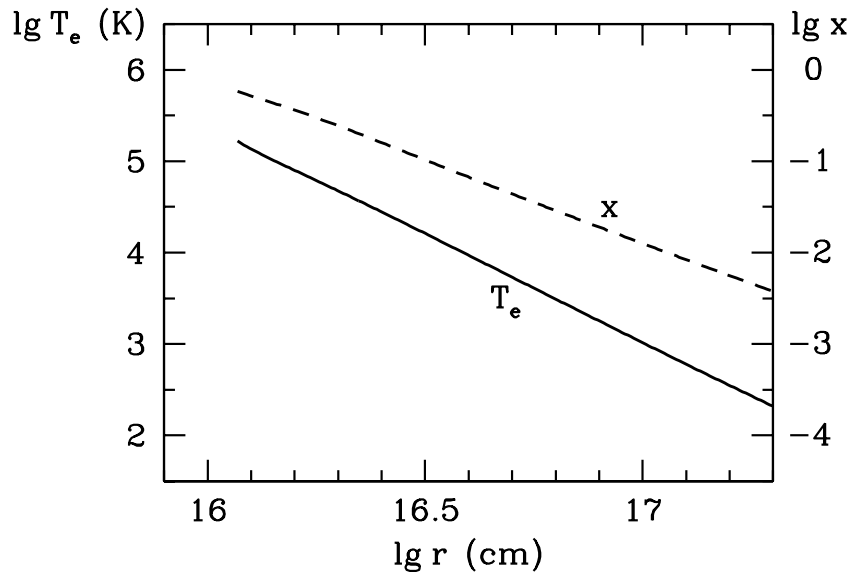


Fig. 2.— Ionization fraction and temperature in the wind on day 30 after the supernova explosion for the wind density parameter $\omega = 0.1$.

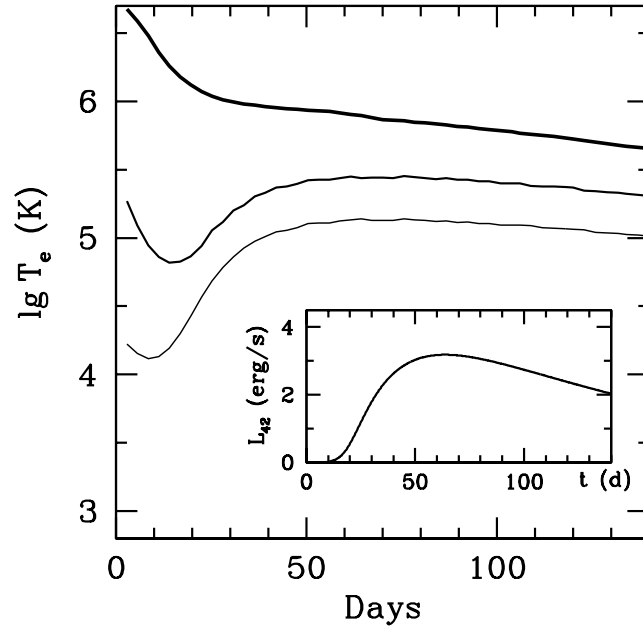


Fig. 3.— Preshock temperature in the wind for three values of the wind density parameter $\omega = 0.01, 0.1, \text{ and } 1$. The line thickness grows with the density. The inset shows the evolution of the luminosity of escaping gamma-rays in units of $10^{42} \text{ erg s}^{-1}$.

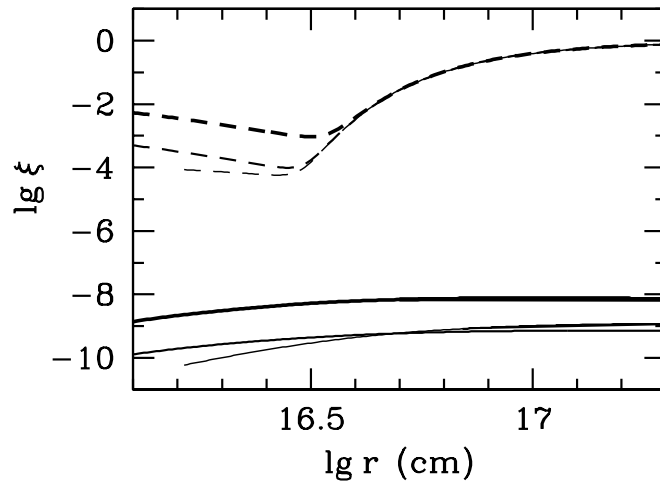


Fig. 4.— The ionization fraction of Na I (*solid line*) and Ca II on day 30 after the supernova explosion for three values of the wind density parameter $\omega = 0.01, 0.1, \text{ and } 1$. The line thickness grows with the density.

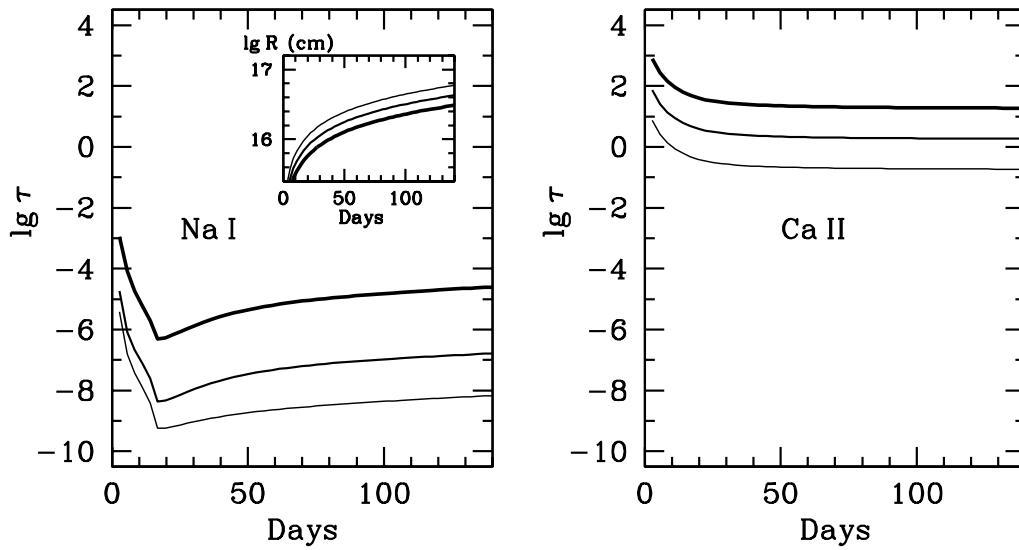


Fig. 5.— The model evolution of the optical depth in the Na I 5890 Å (left) and Ca II 3934 Å (right) for three values of the wind density parameter $\omega = 0.01, 0.1, 1$. The line thickness grows with the density. The inset shows the evolution of the radius of the SN-wind interface for the wind densities indicated above.

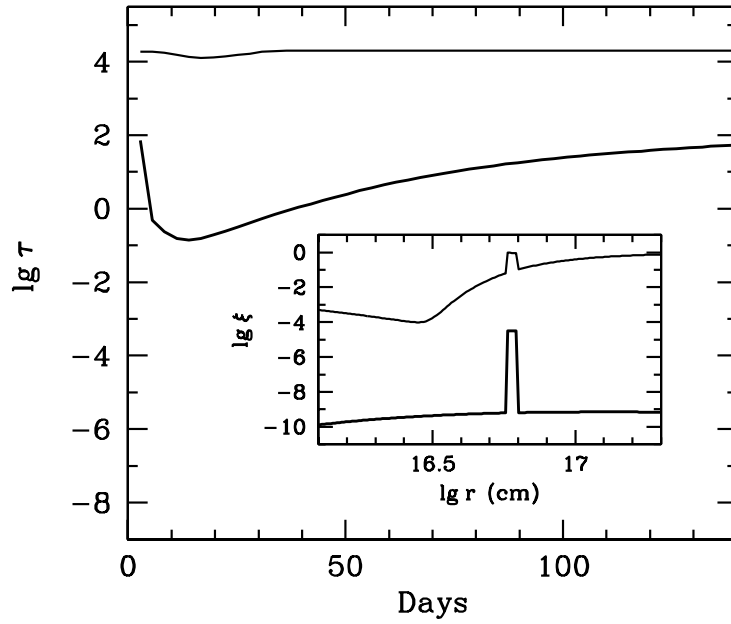


Fig. 6.— The model evolution of the optical depth in the NaI 5890 Å (*thick line*) and CaII 3934 Å for the wind density parameter $\omega = 0.1$ in the case of the dense shell at the distance $r = 6 \times 10^{16}$ cm. The inset shows the radial dependence of the fraction of NaI (*thick line*) and CaII on day 30 after the supernova explosion.